JOC The Journal of Organic Chemistry

Article

pubs.acs.org/joc

Asymmetric Enamine Catalysis with β-Ketoesters by Chiral Primary Amine: Divergent Stereocontrol Modes

Changming Xu, Long Zhang, and Sanzhong Luo*

Beijing National Laboratory for Molecular Sciences (BNLMS), CAS Key Laboratory of Molecular Recognition and Function, Institute of Chemistry, Chinese Academy of Sciences, Beijing 100190, China

Collaborative Innovation Center of Chemical Science and Engineering (Tianjin), Tianjin 300071, China

Supporting Information

ABSTRACT: α-Branched ketones remain a challenging type of substrates in aminocatalysis due to their congested structures as well as the associated difficulties in controlling chemo- and stereoselectivity. In this work, we have explored asymmetric aminocatalysis with α-substituted β-ketoesters. A simple chiral primary amine catalyst was identified to enable unprecedentedly effective catalysis of β-ketoesters in α-hydrazination and Robinson annulation reaction with good yields and high enantioselectivities. Stoichiometric experiments with preformed enamine ester intermediates revealed their enamine-catalytic nature as well as the critical roles of acidic additives in facilitating catalytic turnovers and in tuning the chemo- and stereoselectivity. With the identical catalytic system, the two reactions demonstrated opposite chiral inductions in terms of the absolute configurations of the newly formed stereogenic centers. Investigations into this intriguing issue by DFT have revealed divergent stereocontrol modes. For α-hydrazination, H-bonding-directed facial attack determines the stereoselectivity, whereas a steric model is applied to the Robinson annulation where dual activations of both β-ketoester and vinyl ketone/aldehyde are involved.

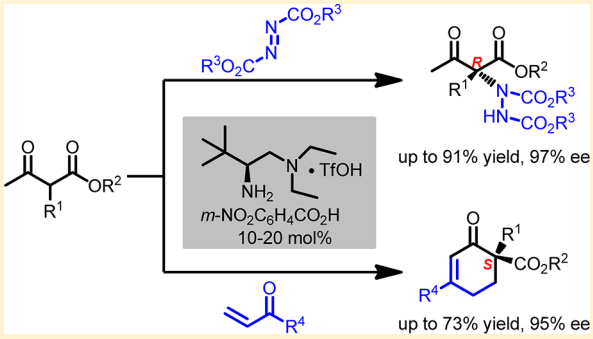

INTRODUCTION

With enamine catalysis stepping into its second decade ever since its renaissance, scopes of studies have now included either un-, mono-, or disubstituted enamine intermediates in a number of C−C or C−X bond-forming reactions. Though extensively explored, the reaction with α-branched ketones via trisubstituted enamines, an appealing process to access chiral ketones bearing α-quaternary stereogenic carbons, has yet to be realized (Scheme 1).[1] Presumably, the challenges can be understood by considering the sterically hindered nature of α-branched ketones and the issues in controlling the geometry of the forming enamines as well as in steering selectively the subsequent bond formations.

Recently, we have explored the aminocatalysis with acyclic β-ketocarbonyls, wherein asymmetric catalysis via a trisubstituted enamine was pursued.[2] Though well explored as latent enol-type nucleophiles in many catalytic asymmetric transformations, acyclic β-ketocarbonyls as versatile ketone synthons have not been used in iminium/enamine catalysis so far. The idea of aminocatalytic turnover with β-ketocarbonyls also seems counterintuitive because it is also known that amines tend to form stabilized enamines with β-ketoesters as a result of intramolecular H-bonding. In fact, enaminone carbonyls derived from chiral primary amines have been reported as readily preformed nucleophiles in asymmetric synthesis.[3] Synthetic enaminones have been successfully used as the haptens to induce the evolution of antibody aldolases (Scheme 1).[4] As a continuation to our efforts in primary aminocatalysis,[5] we have explored chiral primary amines in the catalysis with acyclic β-ketoesters.[2] In this paper, we present a full account on our efforts in exploring the aminocatalysis with β-ketoesters in the α-amination as well as Robinson-type annulation reactions. Our detailed mechanistic studies have revealed divergent stereocontrol modes for the same primary amine catalyst.

Scheme 1. Overview of Enamine Catalysis

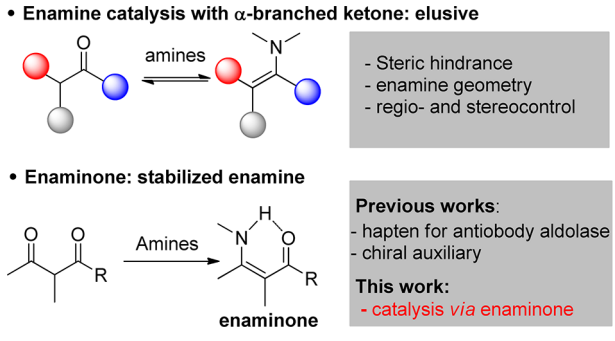

Received: September 19, 2014
Published: November 4, 2014

RESULTS AND DISCUSSION

α-Amination. Recently, we reported a chiral primary amine catalyzed α-amination of β-ketocarbonyls wherein an enamine catalytic cycle was successfully telescoped with Cu(I)-mediated aerobic oxidation of *N*-hydroxycarbamate.[2a] The reactions occurred smoothly under aerobic conditions to give the amination adducts with excellent enantioselectivities, thus providing a facile route for the synthesis of α-quaternary amino acids (Scheme 2). In this process, it was found that the

Scheme 2

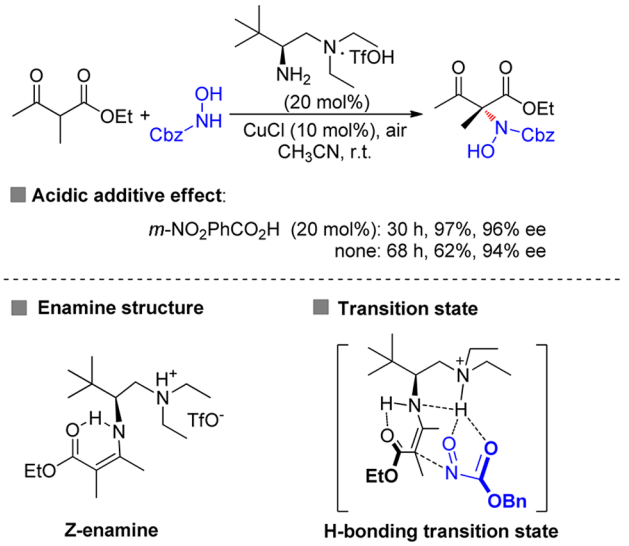

challenging issue on catalytic turnover with an enaminone intermediate could be addressed by judiciously tuning multi-acidic additives, consistent with the known acidic effects in aminocatalysis as well as our previous studies in primary amine catalysis.[6] In addition, the catalytically active enamine intermediate was determined to be mainly in the *Z*-configuration in both solid and solution phase. The H-bonding network involving the protonated tertiary amine moiety as well as the enamine N−H in this *Z*-enamine would stereoselectively guide the approach of electrophile, e.g., nitrosocarbonyl, accounting for the high chemo- and stereoselectivity observed experimentally (Scheme 2).[2b]

Parallel to the work on oxidative amination, we have also investigated the direct α-hydrazination of β-ketoesters with readily available electrophilic azodicarboxylates. The same reaction has been extensively explored with Lewis acid catalysis,[7] H-bond catalysis,[8] and phase-transfer catalysis.[9] Unfortunately, most of the organocatalytic reactions are limited to cyclic β-ketoesters, and the attempts with acyclic β-ketoesters normally gave poor enantioselectivities.[8,9] Recently, the Deng group has reported an enantioselective α-hydrazination of acyclic β-ketoesters but with thioester derivatives.[10]

Our previously developed primary amines were quickly found to be viable catalysts for the reaction of acyclic β-ketoester **1a** and dibenzyl azodicarboxylate **2a**. The catalyst **3a** derived from *tert*-leucine, an optimal catalyst in the oxidative amination reaction, was identified to be the optimal catalyst for asymmetric α-hydrazination of acyclic β-ketoester **1a**. The desired adduct was isolated with 91% yield and 95% ee in dichloromethane (Table 1, entry 1). The use of other catalysts (e.g., **3b**−**e**) also led to high enantioselectivities but moderate

Table 1. Screening and Optimization for α-Hydrazination of β-Ketoesters[a]

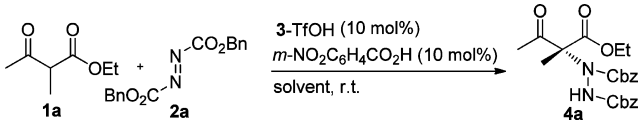

entry	catalyst	solvent	time (h)	yield[b] (%)	ee[c] (%)
1	**3a**	CH_2Cl_2	30	91	95
2	**3b**	CH_2Cl_2	40	68	95
3	**3c**	CH_2Cl_2	72	50	87
4	**3d**	CH_2Cl_2	80	55	91
5	**3e**	CH_2Cl_2	72	74	92
6	**3a**	MeCN	96	93	91
7	**3a**	THF	40	37	94
8	**3a**	Et_2O	48	52	94
9	**3a**	toluene	48	73	95
10	**3a**	MeOH	30	14	81

[a]The reactions were performed at room temperature in 0.2 mL solvent with **1a** (0.10 mmol), **2a** (0.12 mmol), **3**-TfOH (10 mol %) and *m*-nitrobenzoic acid (10 mol %). [b]Isolated yields. [c]Determined by chiral HPLC.

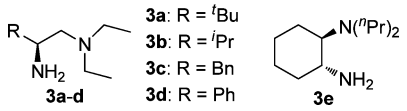

yields (Table 1, entries 2−5). Further optimization revealed that dichloromethane is the solvent of choice (Table 1, entries 6−10). To the best of our knowledge, the current primary aminocatalyst furnishes so far the best outcome in organocatalytic α-hydrazination of acyclic β-ketoesters.

The scope of the α-hydrazination was next explored. As shown in Table 2, acetoacetates **1** with ethyl, methyl, as well as butyl ester can be equally applied in the reactions to afford the desired adducts in high yields and excellent enantioselectivities (Table 2, entries 1−3). Substrates bearing sterically bulky *tert*-butyl ester, benzyl ester, unsaturated allyl ester, and α-allyl or propargyl substituents were also smoothly converted to the expected products at 40 °C in moderate yields and high enantioselectivities (Table 2, entries 4−8). Furthermore, the cyclic β-ketoester **1j** can also be employed as a nucleophile to furnish the desired product with 73% yield and 96% ee (Table 2, entry 10). This reaction is also compatible with diethyl azodicarboxylates **2b** as nitrogen source to give the desired amination adducts in high yields and excellent enantioselectivities (Table 2, entries 11 and 12). For bulky β-ketoesters, higher temperature was necessary to speed up the reaction but slightly sacrificed the enantioselectivity. The absolute configuration of the α-hydrazination adducts **4a** and **4j** was determined to be *R* by comparison with the literature.[7b]

Robinson Annulation. Recently, we reported chiral primary amine **3a**−TfOH catalyzed Robinson annulation between 1,3-cyclohexanediones and methyl vinyl ketone (MVK), furnishing a practical protocol for asymmetric synthesis of Wieland−Miescher ketones (1−100 g) (Scheme 3).[11] In this study, we further extended the reaction to acyclic 1,3-diketones, particularly β-ketoesters. This seemingly minor substrate extension turned out to be nontrivial as the reaction involves the creation of an all-carbon quaternary stereogenic center from acyclic substrate, a scenario distinctive from its counterpart with 1,3-cyclohexanediones wherein a cyclic quaternary stereocenter is generated from a desymmetric

dx.doi.org/10.1021/jo502152w | J. Org. Chem. 2014, 79, 11517−11526

Table 2. Asymmetric α-Hydrazination of β-Ketoesters[a,b]

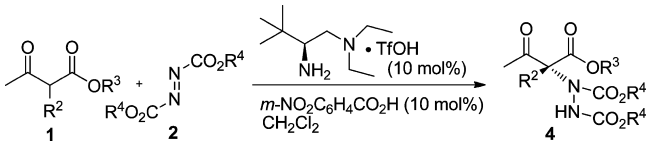

1 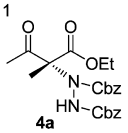 4a r.t., 30 h 91%, 95% ee	2 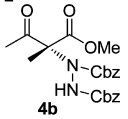 4b r.t., 20 h 88%, 91% ee	3 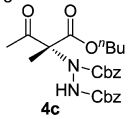 4c r.t., 30 h 70%, 96% ee	4 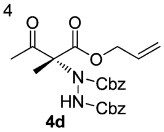 4d 40 °C, 24 h 64%, 74% ee
5 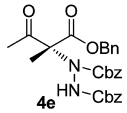 4e 40 °C, 24 h 58%, 74% ee	6 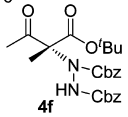 4f 40 °C, 24 h 60%, 82% ee	7[c] 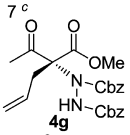 4g 40 °C, 48 h 56%, 87% ee	8[c] 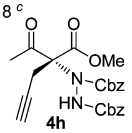 4h 40 °C, 60 h 58%, 55% ee
9 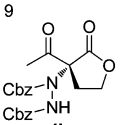 4i r.t., 48 h 90%, 70% ee	10 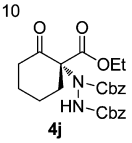 4j r.t., 40 h 73%, 96% ee	11 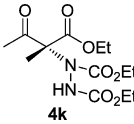 4k r.t., 60 h 78%, 94% ee	12 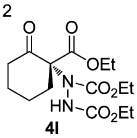 4l r.t., 18 h 88%, 97% ee

[a]The reactions were performed at room temperature in 0.2 mL of CH_2Cl_2 with **1** (0.10 mmol), **2** (0.12 mmol), **3a**–TfOH (10 mol %), and *m*-nitrobenzoic acid (10 mol %). [b]Isolated yields. [c]Reaction conducted with 0.15 mmol of **2a**.

Scheme 3

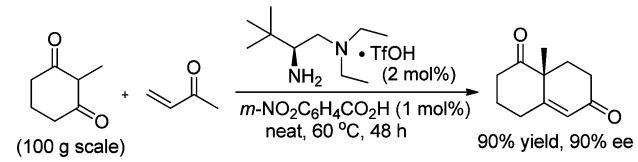

aldol condensation. In addition, as both ketoesters and vinyl ketones are amenable to aminocatalysis, there would be two competing reaction pathways (**I** and **II**) leading to two annulation adducts (e.g., **6a** and **7**, Scheme 4), respectively, hence adding further challenges to the Robinson annulation of β-ketoester and MVK. In fact, such a reaction with acyclic β-ketoesters has not been achieved in organocatalysis in spite of the prevalence of aminocatalysis.[3a,12−14]

Scheme 4

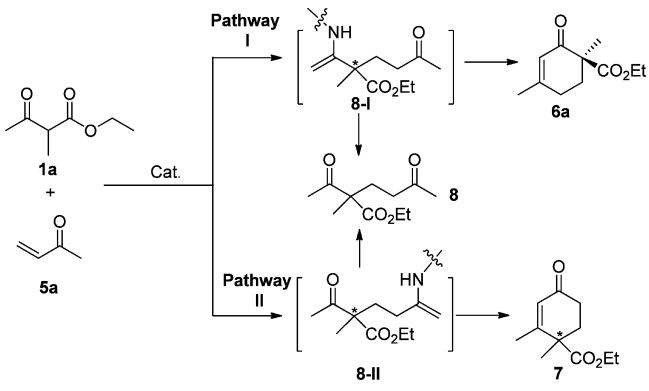

In order to further extend the scope of aminocatalysis with β-ketoesters, we have explored the Robinson annulation with MVK. Initially, the reaction of β-ketoester **1a** and MVK catalyzed by primary amine **3a**–TfOH was found to give **7** with moderate yield and low enantioselectivity (Table 3, entry 1). Interestingly, the addition of a second weak acid, *m*-nitrobenzoic acid, led to the isolation of **6a** with high enantioselectivity (Table 3, entry 2). Further increasing the loading of *m*-nitrobenzoic acid favored the formation of **6a**, with a concurrent reduction in **7** (Table 3, entry 3 vs 2). The dramatically different chiral induction observed with **6a** and **7** is a clear indication of two competing reaction pathways in this reaction system. Conditions were then searched in order to suppress the unselective **7**-forming process. It was soon discovered that portionwise addition of MVK to maintain an excess β-ketoester **1a** in the reaction mixture was in favor of the formation of **6a** (Table 3, entry 4). The screening of different solvents was then followed, and the reaction was found to afford only product **6a** with 54% yield and 94% ee in CH_3CN; no **7** could be isolated in this case (Table 3, entry 9). In other solvents, adduct **7** was generally isolated in varied amounts (Table 3, entries 5−12); occasionally, uncyclized product **8**, a likely precursor for **7**, was isolated. Both **7** and **8** were determined to be of low enantioselectivities (Table 3, entries 5 and 10). Finally, the yield of **6a** could be significantly improved by syringe pump addition of MVK (Table 3, entries 13 and 14).

Under the optimal conditions, we then examined the substrate scope of this Michael−aldol domino reaction. Both MVK and acrolein **5b** could be employed as Michael acceptors to furnish the target products with moderate yields and high to excellent enantioselectivities (Table 4, entries 1−5). However, when the R^2 substituent of acetoacetates was changed to larger group ^{n}Pr, the yield declined dramatically, but the enantioselectivity was maintained (Table 4, entry 6). Other substrates bearing a bulky group (e.g., Bn and ^{t}Bu) in either the R^2 or R^3 position gave poor outcomes (<20% yield).

The absolute configuration of the cyclized product **6a** was determined to be *S*- from the X-ray structure of *p*-bromobenzoylhydrazone derivative **9** (Figure 1), which was opposite to the absolute configuration of α-hydrazination and α-hydroxyamination products of β-ketoesters. This unexpected stereoinduction is strongly suggestive of a distinctive catalytic mode in the reaction.

■ MECHANISTIC STUDIES

With the established catalysis with β-ketoesters, we then carried out detailed experimental and theoretical studies for better understanding of the mechanism. Specifically, the synthesis of enamine ester intermediates, their stoichiometric reactions, as well as the origins of stereocontrols were investigated with our identified optimal catalyst.

1. Stoichiometric Chemistry of Enamine Ester Intermediates. *Synthesis and Characterization of Enamine Ester Intermediates.* It was found that a catalytic amount of *m*-nitrobenzoic acid could effectively promote the stoichiometric reactions of acetoacetates **1** and chiral primary amine **3a** to give the expected enamine esters (Table 5, entry 1 vs 2). After quick filtration on a basic alumina column, the enamine esters **10** could be obtained as analytically pure compounds. As shown in Table 5, there seems to be virtually no obstacle to forming enamine with β-ketoesters bearing bulky ester groups (entries

dx.doi.org/10.1021/jo502152w | J. Org. Chem. 2014, 79, 11517−11526

Table 3. Optimization for Robinson Annulation

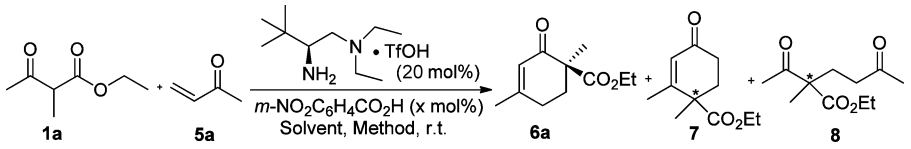

1a 5a 6a 7 8

				yield[b]/ee[c] (%)		
entry	method[a]	solvent	x	**6a**	**7**	**8**
1	A	neat	0	trace	51/23	
2	A	neat	10	10/80	29/4	
3	A	neat	20	18/89	15/24	
4	B	neat	20	54/95	28/20	
5	B	DCM	20	14/84	5/63	17/61
6	B	THF	20	16/81	21/37	trace
7	B	Et_2O	20	21/90	16/30	trace
8	B	toluene	20	46/82	21/30	trace
9	B	MeCN	20	54/94	trace	
10	B	MeOH	20	7/94	49/4	5/5
11	B	DMF	20	10/81	46/−11	trace
12	B	DMSO	20	13/83	41/−23	trace
13	C	MeCN	20	26/94	trace	14/43
14[d]	C	MeCN	20	73/95	trace	

[a]Method A: reactions were performed for 60 h with **1a** (0.2 mmol), MVK (0.24 mmol), catalyst **3a**−TfOH (20 mol %), and *m*-nitrobenzoic acid (0−20 mol %). Method B: MVK (0.2 mmol) was added in portions (one-fifth every 6 h) into the mixture of **1a** (0.4 mmol), catalyst **3a**-TfOH (20 mol %), and *m*-nitrobenzoic acid (20 mol %) in solvent (0.3 mL). Method C: MVK (0.2 mmol) was dissolved in MeCN (0.3 mL) and slowly added into the mixture of **1a** (0.4 mmol), catalyst **3a**−TfOH (20 mol %), *m*-nitrobenzoic acid (20 mol %), and MeCN (0.2 mL) using a syringe pump for 20 h. [b]Isolated yields. [c]Determined by chiral HPLC. [d]The reaction was performed for 60 h.

Table 4. Michael−Aldol Domino Reactions[a]

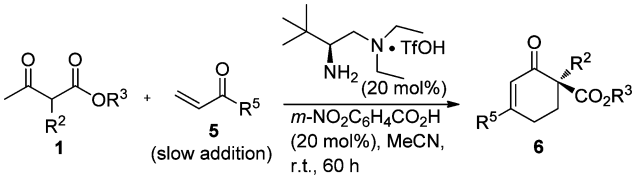

1 5 6

entry	R^2	R^3	R^5	yield[b] (%)	ee[c] (%)
1	Me	Et	Me	73 (68)[d] (**6a**)	95 (95)[d]
2	Me	Me	H	71 (**6b**)	93
3	Et	Me	H	63 (**6c**)	89
4	Et	Et	H	56 (**6d**)	95
5	Me	Et	H	65 (**6e**)	95
6	^{n}Pr	Et	H	31 (**6f**)	93

[a]All reactions were performed at room temperature in 0.5 mL of MeCN with **1** (0.4 mmol), MVK or acrolein (0.2 mmol dissolved in 0.3 mL MeCN, slow addition using syringe pump), **3a**−TfOH (20 mol %), and *m*-nitrobenzoic acid (20 mol %) for 60 h. [b]Isolated yields. [c]Determined by chiral HPLC. [d]1.0 mmol scale reaction.

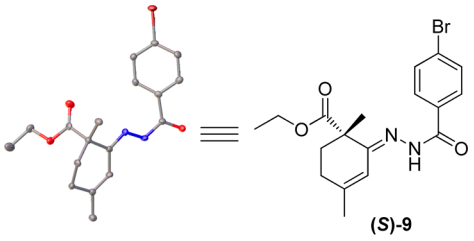

Figure 1. X-ray crystal structure for compound **9**. H atoms are omitted for clearance; thermal ellipsoids set at 30%.

Table 5. Synthesis of Trisubstituted Enamine Intermediates[a]

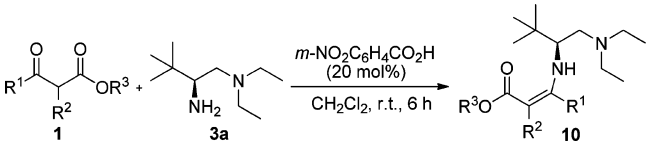

1 3a 10

entry	R^1	R^2	R^3	yield[b] (%)
1	Me	Me	Et	87 (**10a**)
2[c]	Me	Me	Et	28 (**10a**)
3	Me	Me	Me	85 (**10b**)
4	Me	Me	Bn	76 (**10c**)
5	Me	Me	^{t}Bu	43 (**10d**)
6	Me	Bn	Me	67 (**10e**)
7	Me	allyl	Me	65 (**10f**)
8	$(CH_2)_4$		Et	78 (**10g**)
9	Et	Me	Me	20 (**10h**)
10[d]	Et	Me	Me	47 (**10h**)

[a]All reactions were performed at room temperature in 0.5 mL of CH_2Cl_2 with **1** (0.2 mmol), **3a** (0.21 mmol), and *m*-nitrobenzoic acid (20 mol %) for 6 h. [b]Isolated yields. [c]In the absence of *m*-nitrobenzoic acid. [d]Reaction was conducted for 48 h.

3−5). Furthermore, when R^2 was changed to a larger group, such as Bn or allyl, the reaction occurred smoothly with slightly reduced isolated yields (entries 6 and 7). It was noted that cyclic *β*-ketoester, though completely in its enol form as observed by ^{1}HNMR, also underwent enamine formation with catalyst **3a** to give the desired enamine ester **10g** in 78% yield (entry 8). However, ethyl ketone (R^1 = Et) reacted very slowly, and the expected enamine ester **10h** was obtained in only 47% yield after 48 h (entries 9 and 10). The observed reactivity trend is consistent with the respective catalytic behaviors.

dx.doi.org/10.1021/jo502152w | J. Org. Chem. 2014, 79, 11517−11526

Stability of Enamine Intermediates. The stability of enamine ester is considered an unfavorable feature for enamine turnover with ketoesters. During the purification of enamine esters **10**, we noticed that the enamines **10** were rather unstable and underwent facile hydrolysis in the presence of silica gel. Indeed, when the synthesized enamine **10a** was treated with TfOH/*m*-NO_2PhCOOH, complete hydrolysis was observed by NMR.[2a] These observations indicated the catalytic turnover with enamine esters should not be an issue under our catalytic conditions.

Stoichiometric Reactions. The reactivity of enamine **10a** was then examined in this Michael–aldol domino process with MVK. There was no reaction between enamine **10a** and MVK in the absence of acidic additives (Scheme 5, A, entry 1). The

Scheme 5. Control Reactions of Enamine Intermediates 10a with MVK (A) or 2a (B)

(A)

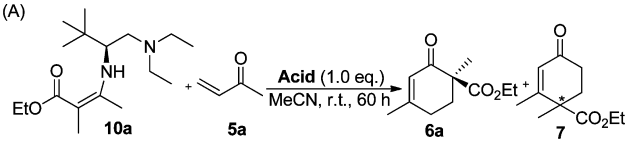

Entry	Acid	6a	7
1	none	0	0
2	TfOH only	15%, 94% ee	53%, 18% ee
3	*m*-$NO_2C_6H_4CO_2H$ only	31%, 40% ee	35%, 13% ee
4	TfOH/*m*-$NO_2C_6H_4CO_2H$	67%, 94% ee	0

(B)

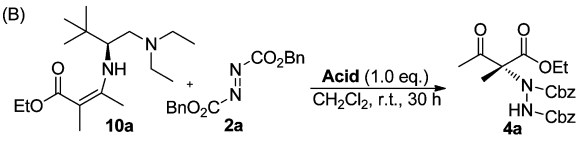

Entry	Acid	4a
1	none	0
2	TfOH only	64%, 93% ee
3	*m*-$NO_2C_6H_4CO_2H$ only	68%, 73% ee
4	TfOH/*m*-$NO_2C_6H_4CO_2H$	82%, 96% ee

addition of either strong acid TfOH or weak acid *m*-nitrobenzoic acid was found to facilitate the reaction, and both **6a** and **7** were isolated in these cases. Notably, in the presence of TfOH high enantioselectivity (94% ee) was achieved for **6a** but not for **7**, although the latter was obtained as the major adduct (A, entries 2 and 3). Consistent with the catalytic behavior, the joint use of TfOH and *m*-nitrobenzoic acid can suppress the formation of **7**, leading to sole production of **6a** in high enantioselectivity (A, entry 4). A similar acidic additive effect has also been observed in the stoichiometric reaction of enamine ester **10a** with dibenzyl azodicarboxylate **2a** (Scheme 5, B).

2. Origin of Stereoselectiviy. A close inspection revealed that the chiral inductions in the two examined reactions are opposite in the sense of the absolute configurations (**4a** vs **6a**), though the same catalytic system was applied in both cases (Figure 2). This intriguing stereocontrol issue was then further investigated by DFT calculations with the Gaussian 09 program package.[15] The recently developed M06-2X functional[16] together with the 6-31G(d) basis set were used for the geometry optimizations and vibrational calculations. Each geometry was confirmed as a minimum (no imaginary

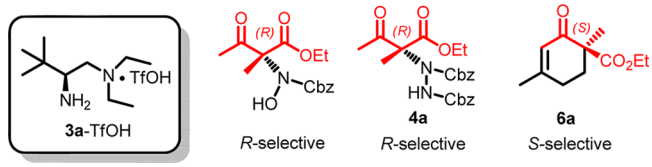

Figure 2. Opposite chiral inductions in hydrazination and Robinson annulation reaction.

frequency) or a transition state (one imaginary frequency) by calculation of harmonic vibrational frequencies. The SMD continuum solvation model[17] with acetonitrile as the solvent were used in single-point energy calculations, and these calculations were performed at the M06-2*x*/6-311+G(d,p) level with gas-phase optimized structures.

Origins of Stereoselectivity for α-Hydranization Reaction. The absolute configuration of the hydranization adduct, e.g., **4a**, was determined to be the same as with the *α*-amination adduct derived from nitrosocarbonyls (Figure 2). Previously, we have found the major *R*-product was formed *via Re*-facial attack to *Z-s-trans* enamine, the most stable enamine intermediate with *β*-ketoesters, while the *Si*-facial addition to *E-s-trans* enamine led to minor *S*-product.[2b] This model has also been tested in the current hydranization reaction with dimethyl azodicarboxylate as the model substrate. The computed free energy difference between these two transition states is 5.9 kcal/mol favoring the formation of *R*-product, in agreement with the experimental observation (Figure 3).

Origins of Stereoselectivity for Robinson Annulation. (1) Reaction Pathway. As both *β*-ketoesters and MVK are amenable to aminocatalysis, the possible reaction pathways were first analyzed. Accordingly, the reaction may be initialized via enamine activation of *β*-ketoesters (Scheme 6, pathway I) to

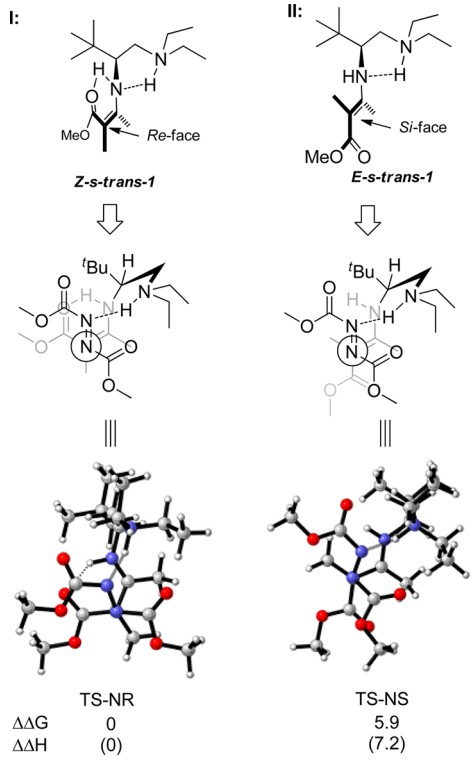

Figure 3. Amination transition states.

dx.doi.org/10.1021/jo502152w | J. Org. Chem. 2014, 79, 11517–11526

Scheme 6. Proposed Catalytic Cycle for the Michael–Aldol Cascade Reactions

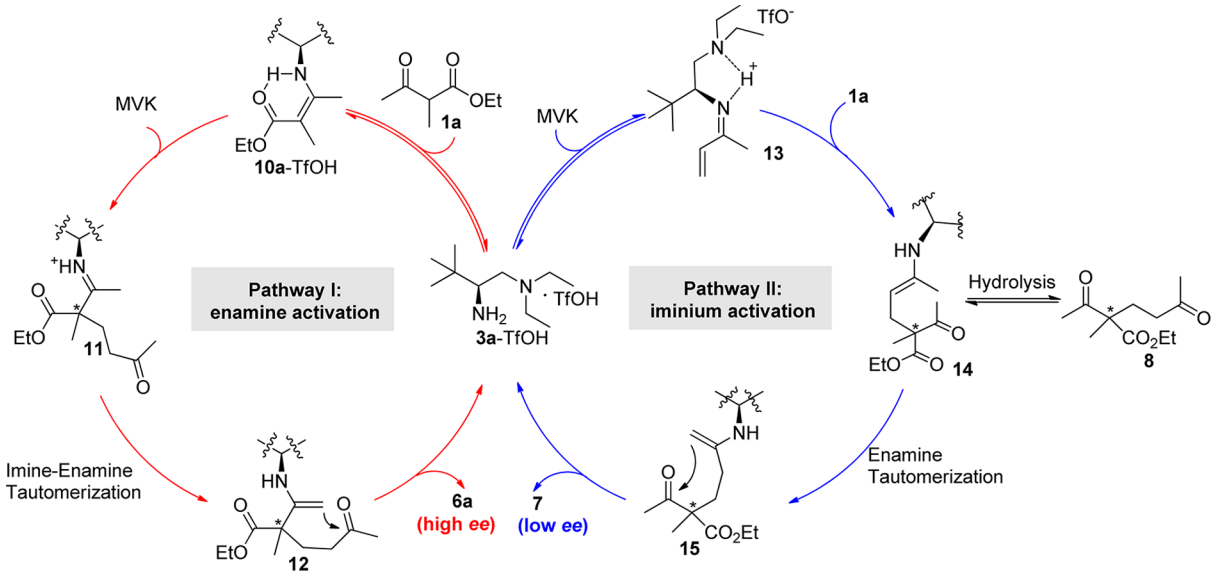

give **6a** or competitively via iminium ion activation of MVK to give **7** (Scheme 6, pathway II). Compounds **6a** and **7** may also be formed from two bifurcating pathways with a common intermediate. However, this possibility can be ruled out as **6a** and **7** are generally obtained in dramatically different enantioselectivities indicating two competitive pathways. The fact that slow addition of MVK can suppress the formation of **7** is in line with the proposed mechanistic scenario (Scheme 6). It is noted that when MVK was added in one portion, only **7** was formed with low ee (Table 3, entry 1), indicating that the formation of iminium ion **13** is much faster than the formation of enamine **10a** and the iminum cycle is a less enantioselective pathway. However, the slow addition of MVK by syringe pump to the reaction system ensured the prior formation of enamine **10a**; thus, the enamine catalytic cycle could dominate in the reaction.

The enamine catalytic nature as well as the critical roles of acidic additives has also been verified by the stoichiometric experiments. A sole production of **6a** in the presence of both TfOH and *m*-nitrobenzoic acid (Scheme 5, A) clearly indicates that the use of combined acids significantly facilitate the enamine coupling in preference to enamine hydrolysis as well as the subsequent iminium activation of MVK. The formation of **7** with either TfOH or *m*-nitrobenzoic acid only was probably caused by the partial hydrolysis of the enamine as well as the participation of iminium catalytic cycle under the conditions. In addition, a linear Michael adduct **8**, derived from either intermediate **11**/**12** or **14**/**15**, has also been isolated. Under the catalytic conditions, the cyclization of **8** proceeded smoothly to furnish **7** as a sole adduct without any enantioselectivity enrichment (Scheme 7). This observation

Scheme 7. Intramolecular Aldol Reactions of Compound 8

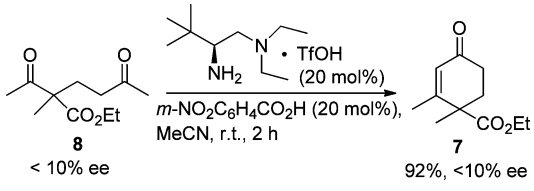

together with the low enantioselectvity of **7** and **8** indicates that the formation of side product **8** is coupled with the nonselective iminium cycle (pathway II) and that product **6a** could only come from the enamine catalytic sequence wherein the initial Michael addition is the critical stereogenic C–C forming step (pathway I).

(2) Initial Explorations on Stereocontrol. The stereocontrol in the enamine cycle for cyclohexenone (*S*)-**6** was then explored by DFT calculations. Following the successes in *α*-oxidative amination and *α*-hydrazination reactions, the H-bonding mode (Figure 4, **I**) involving the protonated

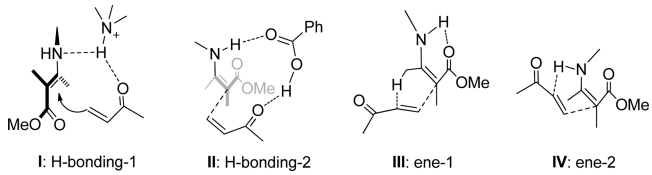

Figure 4. Possible *S*-selective modes for (*S*)-**6a** formation.

ammonium moiety was first considered. Accordingly, we have successfully located all the possible transition states corresponding to *Re*-facial attack and *Si*-facial attack onto enamine intermediates. In this regard, only enamine intermediates with the lowest free energy were considered in the calculations (for a full list of all the possible enamine intermediates, see the Supporting Information). Unexpectedly, the *Re*-facial attack TS was found to be significantly favored over those *Si*-facial attack by >2.0 kcal/mol, leading to *R*-selective product, which is against the experimental observation. Other possible *Si*-facial modes were hence explored, and these include bidentate H-bonding with acid (mode II) and enelike processes III and IV (Figure 4). Unfortunately, all these *S*-selective TSs are disfavored by >3.7 kcal/mol over the *R*-selective TS (see the Supporting Information for details), indicating they are not able to account for the observed *S*-selectivity (Figure 5).

(3) Dual Aminocatalytic Mode. At this point, we reinvestigated the presumed one-catalyst participation mode. The nonlinear effect (NLE) study of the model reaction was performed. As shown in Figure 6, a positive NLE was observed,

dx.doi.org/10.1021/jo502152w | J. Org. Chem. 2014, 79, 11517–11526

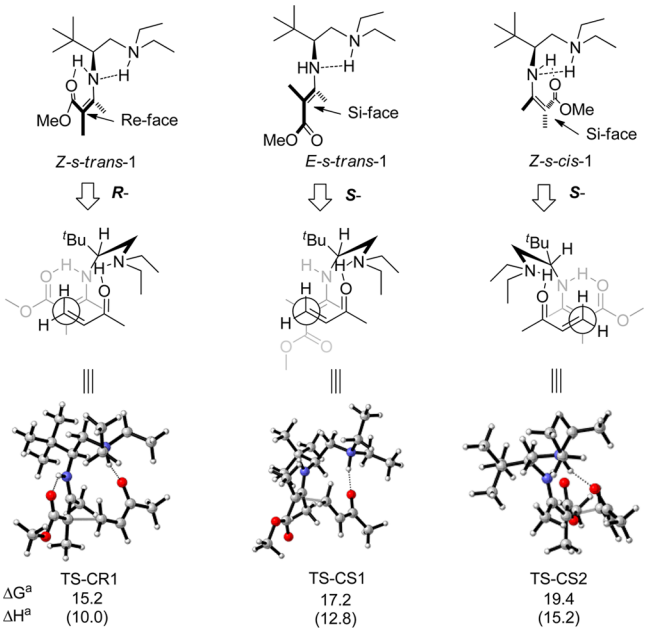

Figure 5. Transition states with H-bonding activated electrophiles (mode I, energies in kcal/mol).

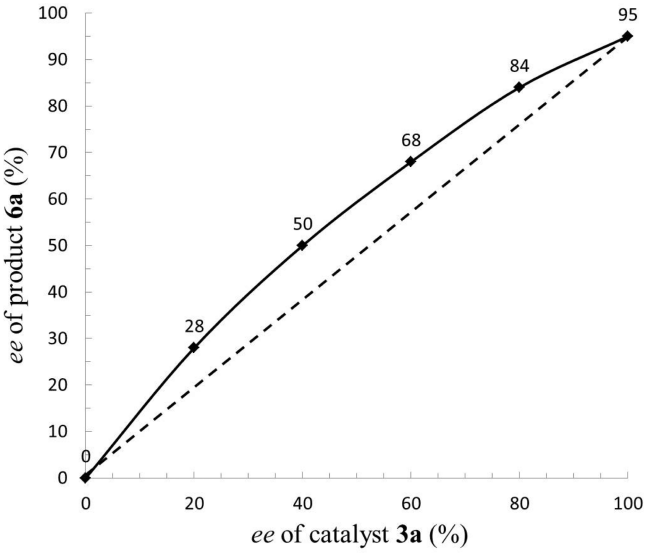

Figure 6. Nonlinear effects of Robinson annulation.

which indicated that more than one molecule of catalyst **3a**−TfOH was likely to be involved in the transition state. Provided with the tendency of MVK undergoing iminium activation, we invoked a dual aminocatalytic mode wherein two in situ generated active species, i.e., enamine ester (e.g., **10a**) and iminium ion (e.g., **13**), derived from two catalyst molecules, respectively, are coupled to forge the critical C−C bond. In this scenario, the critical enamine addition may become sterics-guided instead of H-bonding-directed as proven in the *α*-amination reaction, and the *Si*-facial attack may thus be rendered a favored pathway (Figure 7). Similar dual catalysis has recently been reported in a related Robinson-type reaction wherein a chiral secondary amine in concert with a stoichiometric amount achiral primary amine was reported to fulfill the desired catalysis with good enantioselectivity (Scheme 8).[18]

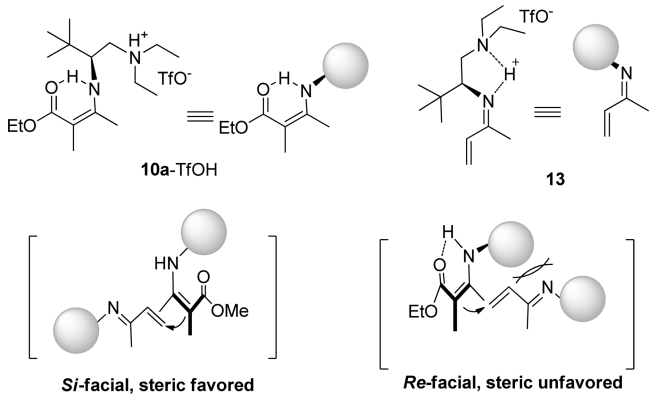

Figure 7. Dual aminocatalytic mode for stereocontrol.

Scheme 8

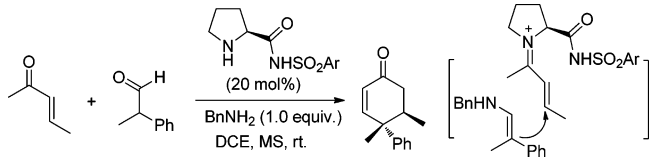

To verify the dual catalysis, we investigated the stereogenic C−C bond formation using enamine **10a**−TfOH and **13** as the coupling components. The two most favored orientations of iminium ion were considered, and we have obtained all four TSs corresponding to the respective *Re*- or *Si*-facial additions. It is noted that all these dual-activation TSs are of much lower activation energy that those of sole enamine catalysis (Figure 8 vs Figure 5), indicating the dual catalysis is a favored reaction pathway. More delightfully, *Si*-facial attack TS is now favored over *Re*-TS by 3.2 kcal/mol, corresponding to 99% ee favoring the *S*-product, which is in accordance with the experimental results.

On the basis of the above results, the initial proposed catalytic cycle was revised as follows (Scheme 9). The target product **6a** was formed by the coupling of enamine **10a**−TfOH and imine **13** via an enamine−imininium dual catalytic process, and the tautomerization of imine intermediate **11** to enamine intermediate **12** led to the formation of **6a**.

■ CONCLUSIONS

In conclusion, chiral primary amine catalyzed *α*-hydrazination and Robinson-type annulation of *β*-ketoesters have been developed. This unprecedented enamine catalysis of *β*-ketoesters is enabled by a simple chiral primary amine derived from *tert*-leucine in concert with a strong acid, TfOH, and a weak acid, *m*-nitrobenzoic acid. The joint use of two acidic additives is critical to facilitate the catalytic turnover and to tune the chemo- and stereoselectivity. Our experimental and theoretical studies have revealed distinctively divergent stereocontrol modes for the same catalytic system, wherein the *α*-hydrazination reaction follows the typical H-bonding model and the Robinson annulation tends to be sterics-guided as a result of its dual-activation nature. This mechanistic scenario sets the basis for future exploration on aminocatalysis with *β*-ketocarbonyls.

■ EXPERIMENTAL SECTION

General Information. Commercial reagents were used as received unless otherwise indicated. ^{1}H and ^{13}C NMR spectra were measured

dx.doi.org/10.1021/jo502152w | J. Org. Chem. 2014, 79, 11517−11526

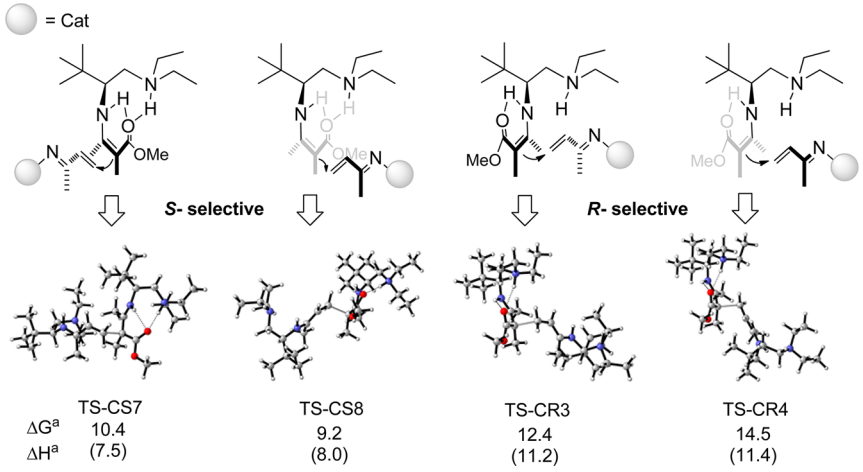

Figure 8. Biactivation transition states (energies in kcal/mol).

Scheme 9. Catalytic Cycle of Robinson Annulation

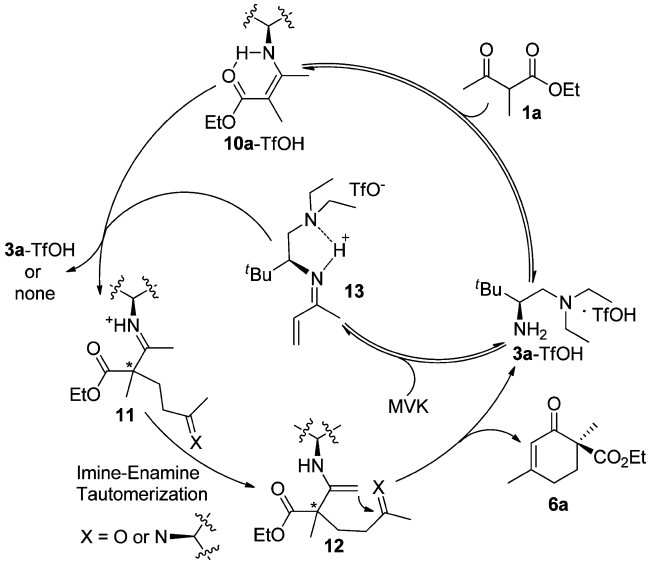

on an NMR instrument (300 and 600 MHz for ^{1}H NMR, 75 MHz for ^{13}C NMR). Tetramethylsilane (TMS) served as the internal standard for ^{1}H NMR, and $CDCl_3$ served as the internal standard for ^{13}C NMR. The enantiomeric excesses were determined by HPLC analysis on AD-H, OD-H, AS-H, OJ-H, and IA columns. Optical rotation was measured on a commercial polarimeter and reported as follows: $[\alpha]^{25}_D$ (c = g/100 mL, solvent). HRMS was measured in ESI mode, and the mass analyzer of the HRMS was orbitrap.

Materials. β-Keto esters **1a**–**f** were prepared by alkylation of the corresponding α-unsubstituted β-keto esters with alkyl iodide.[19] β-Keto ester **1g** was prepared by allylation of the corresponding acetoacetate with allyl bromide.[19] β-Keto esters **1h**[20] and **1j**[21] were prepared according to literature precedent.

General Procedure for the α-Amination of β-Keto Esters. To β-keto ester **1** (0.10 mmol), **3a**–TfOH (10 mol %), and *m*-nitrobenzoic acid (10 mol %) in a standard glass vial with stir bar was added azodicarboxylate **2** (0.12 mmol) followed by CH_2Cl_2 (0.20 mL). The reaction was stirred at room temperature or 40 °C until completion as indicated by TLC. The mixture was directly loaded onto a silica gel column and eluted with ethyl acetate/petroether to give the target products. The products **4a**, **4f**, **4j**–**k**,[7b] and **4i**[8b] are known compounds.

4b: colorless oil, 37.7 mg, 88% yield. $[\alpha]^{25}_D$ = −12.4 (c = 1.0, CH_2Cl_2). HPLC (OD-H, hexane/2-propanol = 4:1, flow rate = 1.0 mL/min, λ = 210 nm): 91% ee, 15.90 min (minor), 17.62 min (major). ^{1}H NMR (300 MHz, $CDCl_3$) δ: 7.32–7.26 (m, 10H), 6.70 (s, 1H), 5.22–5.15 (m, 4H), 3.74 (s, 3H), 2.34 (s, 3H), 1.64 (s, 3H). IR (thin film, cm^{-1}): 3302, 1747, 1731, 1715, 1455. HRMS (ESI): calcd for $C_{22}H_{24}O_7N_2Na^+$ 451.1476, found 451.1473.

4c: colorless oil, 32.9 mg, 70% yield. $[\alpha]^{25}_D$ = −14.0 (c = 1.0, CH_2Cl_2). HPLC (OD-H, hexane/2-propanol = 4:1, flow rate = 1.0 mL/min, λ = 210 nm): 96% ee, 21.65 min (major), 25.50 min (minor). ^{1}H NMR (300 MHz, $CDCl_3$) δ: 7.32–7.26 (m, 10H), 6.65 (s, 1H), 5.22–5.14 (m, 4H), 4.16 (s, 2H), 2.34 (s, 3H), 1.72–1.59 (m, 5H), 1.36–1.31 (m, 2H), 0.91 (t, J = 9 Hz, 3H). IR (thin film, cm^{-1}): 3300, 1738, 1731, 1715, 1455. HRMS (ESI): calcd for $C_{25}H_{30}O_7N_2Na^+$ 493.1945, found 493.1943.

4d: colorless oil, 29.1 mg, 64% yield. $[\alpha]^{25}_D$ = −9.6 (c = 1.0, CH_2Cl_2). HPLC (AD-H, hexane/2-propanol = 4:1, flow rate = 1.0 mL/min, λ = 210 nm): 74% ee, 20.51 min (minor), 25.61 min (major). ^{1}H NMR (300 MHz, $CDCl_3$) δ: 7.32–7.26 (m, 10H), 6.65 (s, 1H), 5.86–5.80 (m, 1H), 5.35–5.14 (m, 6H), 4.65 (s, 2H), 2.34 (s, 3H), 1.67 (s, 3H). IR (thin film, cm^{-1}): 3306, 1738, 1731, 1715, 1498, 1455. HRMS (ESI): calcd for $C_{24}H_{26}O_7N_2Na^+$ 477.1632, found 477.1629.

4e: colorless oil, 29.2 mg, 58% yield. $[\alpha]^{25}_D$ = −12.0 (c = 0.5, CH_2Cl_2). HPLC (OD-H, hexane/2-propanol = 4:1, flow rate = 1.0 mL/min, λ = 210 nm): 74% ee, 18.65 min (major), 22.42 min (minor). ^{1}H NMR (300 MHz, $CDCl_3$) δ: 7.33–7.26 (m, 15H), 6.61 (s, 1H), 5.27–5.08 (m, 6H), 2.31 (s, 3H), 1.65 (s, 3H). IR (thin film, cm^{-1}): 3305, 1731, 1498, 1455. HRMS (ESI): calcd for $C_{28}H_{28}O_7N_2Na^+$ 527.1789, found 527.1784.

4g: colorless oil, 25.4 mg, 56% yield. $[\alpha]^{25}_D$ = −1.2 (c = 0.5, CH_2Cl_2). HPLC (OD-H, hexane/2-propanol = 4:1, flow rate = 1.0 mL/min, λ = 210 nm): 87% ee, 12.10 min (minor), 15.52 min (major). ^{1}H NMR (300 MHz, $CDCl_3$) δ: 7.33–7.26 (m, 10H), 6.63 (s, 1H), 5.83 (s, 1H), 5.15–5.0 (m, 6H), 3.72 (s, 3H), 2.83 (s, 2H), 2.34 (s, 3H), 1.64 (s, 3H). IR (thin film, cm^{-1}): 3305, 1738, 1731, 1498, 1455. HRMS (ESI): calcd for $C_{24}H_{26}O_7N_2Na^+$ 477.1632, found 477.1627.

4h: colorless oil, 26.2 mg, 58% yield. $[\alpha]^{25}_D$ = 2.4 (c = 0.5, CH_2Cl_2). HPLC analysis: (OD-H, hexane/2-propanol = 4:1, flow rate = 1.0 mL/min, λ = 210 nm): 55% ee, 16.04 min (minor), 21.94 min (major). ^{1}H NMR (300 MHz, $CDCl_3$) δ: 7.33–7.26 (m, 10H), 6.82 (s, 1H), 5.17 (s, 4H), 3.78–3.68 (m, 3H), 3.10 (s, 2H), 2.43 (s, 3H), 2.03 (s, 1H). IR (thin film, cm^{-1}): 3290, 2920, 1747, 1731, 1498, 1455. HRMS (ESI): calcd for $C_{24}H_{24}O_7N_2Na^+$ 475.1476, found 475.1470.

4l: colorless oil, 30.3 mg, 88% yield. $[\alpha]^{25}_D$ = −13.6 (c = 1.0, CH_2Cl_2). HPLC (AS-H, hexane/2-propanol = 4:1, flow rate = 1.0 mL/min, λ = 210 nm): 97% ee, 10.86 min (minor), 13.47 min (major). ^{1}H NMR (300 MHz, $CDCl_3$) δ: 6.23 (s, 1H), 4.29–4.13 (m, 6H), 2.91–2.70 (m, 1H), 2.46–2.05 (m, 4H), 1.90–1.53 (m, 3H), 1.31–1.21 (m, 9H). IR (thin film, cm^{-1}): 3295, 1732, 1507, 1218. HRMS (ESI): calcd for $C_{15}H_{24}O_7N_2Na^+$ 367.1476, found 367.1475.

dx.doi.org/10.1021/jo502152w | J. Org. Chem. 2014, 79, 11517–11526

General Procedure for Robinson annulation. To β-keto ester **1** (0.40 mmol), **3a**–TfOH (20 mol %), *m*-nitrobenzoic acid (20 mol %), and MeCN (0.2 mL) in a standard glass vial with stir bar was added **5** (0.2 mmol in 0.3 mL MeCN) slowly using a syringe pump for 60 h at room temperature. Another 3 h later, the mixture was directly loaded onto silica gel column and eluted with ethyl acetate/petroether to give the target products. The products **6a**, **7**,[13] and **8**[14e] are known compounds.

6b: colorless oil, 23.9 mg, 71% yield. $[\alpha]^{25}_{D}$ = 17.6 (*c* = 0.5, MeOH). HPLC (AD-H × 2, hexane/2-propanol = 99:1, flow rate = 0.5 mL/min, λ = 210 nm): 93% ee, 49.19 min (major), 52.70 min (minor). ^{1}H NMR (300 MHz, $CDCl_3$) δ: 6.97–6.85 (m, 1H), 6.04 (dt, *J* = 10.2, 2.0 Hz, 1H), 3.69 (s, 3H), 2.56–2.27 (m, 3H), 1.93–1.87 (m, 1H), 1.39 (s, 3H). ^{13}C NMR (75 MHz, $CDCl_3$) δ 197.0, 173.2, 149.6, 129.0, 53.5, 52.6, 33.4, 23.8, 20.5. IR (thin film, cm^{-1}): 1733, 1682, 1622, 1456, 1258. HRMS (ESI): calcd for $C_9H_{12}O_3Na^+$ 191.0679, found 191.0678.

6c: colorless oil, 22.9 mg, 63% yield. $[\alpha]^{25}_{D}$ = 18.0 (c = 0.5, MeOH). HPLC (AD-H × 2, hexane/2-propanol = 99:1, flow rate = 0.5 mL/min, λ = 210 nm): 89% ee, 44.56 min (major), 50.15 min (minor). ^{1}H NMR (300 MHz, $CDCl_3$) δ: 6.91–6.86 (m, 1H), 6.07–5.96 (m, 1H), 3.69 (s, 3H), 2.59–2.40 (m, 2H), 2.40–2.26 (m, 1H), 2.04–1.88 (m, 2H), 1.85–1.73 (m, 1H), 0.91 (t, *J* = 7.5 Hz, 3H). ^{13}C NMR (75 MHz, $CDCl_3$) δ: 196.5, 172.2, 149.4, 129.4, 57.4, 52.4, 29.6, 26.9, 23.8, 9.2. IR (thin film, cm^{-1}): 1732, 1683, 1622, 1435, 1241. HRMS (ESI): calcd for $C_{10}H_{14}O_3Na^+$ 205.0835, found 205.0835.

6d: colorless oil, 22.0 mg, 56% yield. $[\alpha]^{25}_{D}$ = 24.0 (*c* = 0.5, MeOH). HPLC (AD-H × 2, hexane/2-propanol = 99:1, flow rate = 0.5 mL/min, λ = 210 nm): 95% ee, 39.28 min (major), 43.55 min (minor). ^{1}H NMR (300 MHz, $CDCl_3$) δ: 6.94–6.80 (m, 1H), 6.00 (d, *J* = 9.0 Hz, 1H), 4.15 (q, *J* = 7.1 Hz, 2H), 2.57–2.39 (m, 2H), 2.36–2.24 (m, 1H), 2.01–1.89 (m, 2H), 1.84–1.72 (m, 1H), 1.21 (t, *J* = 7.1 Hz, 3H), 0.91 (t, *J* = 7.5 Hz, 3H).^{13}C NMR (75 MHz, $CDCl_3$) δ: 196.5, 171.7, 149.2, 129.4, 61.2, 57.3, 29.6, 26.8, 23.8, 14.2, 9.1. IR (thin film, cm^{-1}): 1729, 1685, 1622, 1238. HRMS (ESI): calcd for $C_{11}H_{16}O_3Na^+$ 219.0992, found 219.0990.

6e: colorless oil, 23.7 mg, 65% yield. $[\alpha]^{25}_{D}$ = 20.0 (*c* = 0.5, MeOH). HPLC (AD-H × 2, hexane/2-propanol = 99:1, flow rate = 0.5 mL/min, λ = 210 nm): 95% ee, 47.71 min (major), 51.27 min (minor). ^{1}H NMR (300 MHz, $CDCl_3$) δ: 6.95–6.85 (m, 1H), 6.04 (dt, *J* = 10.2, 1.9 Hz, 1H), 4.16 (q, *J* = 7.0 Hz, 2H), 2.55–2.41 (m, 2H), 2.40–2.27 (m, 1H), 1.94–1.83 (m, 1H), 1.38 (s, 3H), 1.22 (t, *J* = 7.1 Hz, 3H). ^{13}C NMR (75 MHz, $CDCl_3$) δ: 197.1, 172.8, 149.4, 129.1, 61.4, 53.5, 33.5, 23.8, 20.5, 14.2. IR (thin film, cm^{-1}): 1730, 1684, 1623, 1456, 1254. HRMS (ESI): calcd for $C_{10}H_{14}O_3Na^+$ 205.0835, found 205.0835.

6f: colorless oil, 13.0 mg, 31% yield. $[\alpha]^{25}_{D}$ = 26.0 (c = 0.5, MeOH). HPLC (AD-H × 2, hexane/2-propanol = 99:1, flow rate = 0.5 mL/min, λ = 210 nm): 93% ee, 43.23 min (major), 51.17 min (minor). ^{1}H NMR (300 MHz, $CDCl_3$) δ: 6.92–6.80 (m, 1H), 6.05–5.95 (m, 1H), 4.15 (q, *J* = 7.1 Hz, 2H), 2.58–2.40 (m, 2H), 2.37–2.26 (m, 1H), 1.99–1.82 (m, 2H), 1.75–1.66 (m, 1H), 1.36–1.25 (m, 2H), 1.21 (t, *J* = 7.1 Hz, 3H), 0.92 (t, *J* = 7.3 Hz, 3H). ^{13}C NMR (75 MHz, $CDCl_3$) δ: 196.5, 171.7, 149.2, 129.3, 61.24, 57.2, 36.0, 30.1, 23.9, 18.0, 14.6, 14.2. IR (thin film, cm^{-1}): 1729, 1685, 1623, 1448, 1226. HRMS (ESI): calcd for $C_{12}H_{18}O_3Na^+$ 233.1148, found 233.1147.

Synthesis of Compound 9. To a solution of compound **6a** (0.3 mmol) in EtOH (10 mL) was added *p*-bromobenzoylhydrazone (0.3 mmol). After being refluxed for 12 h, the mixture was concentrated in vacuo. The residue was loaded on column chromatography and eluted with ethyl acetate/petroether to give the target product **9** (97.6 mg, 83% yield) as a white solid: $[\alpha]^{25}_{D}$ = 153.6 (*c* = 0.5, $CHCl_3$). Mp: 140–142 °C. ^{1}H NMR (300 MHz, $CDCl_3$) δ: 9.15 (s, 1H), 7.82–7.55 (m, 4H), 6.28 (s, 1H), 4.11 (s, 2H), 2.36–2.20 (m, 3H), 1.93 (s, 3H), 1.71 (s, 1H), 1.33–1.19 (m, 6H). IR (thin film, cm^{-1}): 3340, 2927, 1726, 1653, 1589, 1529, 1480, 1254. HRMS (ESI): calcd for $C_{18}H_{21}O_3N_2BrNa^+$ 415.0628, found 415.0623.

Synthesis of Compounds 10a–h. To a round-bottom flask containing β-ketoester **1** (0.20 mmol), chiral primary amine **3a** (0.21 mmol), and CH_2Cl_2 (0.5 mL), was added *m*-nitrobenzoic acid (0.04 mmol). The reaction was stirred at room temperature. After 6 h, the mixture was loaded onto basic alumina and eluted quickly with ethyl acetate/petroether (1:10) to give enamine **10**. Enamine intermediates **10a** and **10c** are known compounds.[2a]

10b: colorless oil, 48.3 mg, 85% yield. ^{1}H NMR (300 MHz, CD_3CN) δ: 9.61 (d, *J* = 9.2 Hz, 1H), 3.59 (s, 3H), 3.31 (td, *J* = 10.3, 2.2 Hz, 1H), 2.68–2.47 (m, 3H), 2.44–2.21 (m, 3H), 2.00 (s, 3H), 1.78 (s, 3H), 0.98–0.89 (m, 15H). ^{13}C NMR (75 MHz, CD_3CN) δ: 172.0, 162.8, 84.7, 62.0, 56.9, 50.5, 48.5, 35.2, 26.9, 16.3, 13.0, 12.5. IR (thin film, cm^{-1}): 2967, 1641, 1601, 1457, 1620. HRMS (ESI): calcd for $C_{16}H_{33}O_2N_2^+$ 285.2537, found 285.2534.

10d: colorless oil, 28.0 mg, 43% yield. ^{1}H NMR (300 MHz, $CDCl_3$) δ: 9.33 (d, *J* = 10.6 Hz, 1H), 3.16 (t, *J* = 10.0 Hz, 1H), 2.61 (dd, *J* = 13.6, 2.0 Hz, 1H), 2.54–2.27 (m, 5H), 1.93 (s, 3H), 1.75 (s, 3H), 1.46 (s, 9H), 0.98–0.90 (m, 15H). ^{13}C NMR (75 MHz, $CDCl_3$) δ: 171.3, 159.9, 86.8, 61.6, 56.2, 48.1, 35.0, 28.8, 28.1, 27.0, 16.2, 13.7, 12.4. IR (thin film, cm^{-1}): 2968, 1638, 1602, 1455, 1272. HRMS (ESI): calcd for $C_{19}H_{39}O_2N_2^+$ 327.3006, found 327.3004.

10e: colorless oil, 48.2 mg, 67% yield. ^{1}H NMR (300 MHz, $CDCl_3$) δ: 9.83 (d, *J* = 10.6 Hz, 1H), 7.30–7.06 (m, 5H), 3.69 (d, *J* = 7.2 Hz, 2H), 3.61 (s, 3H), 3.27–3.14 (m, 1H), 2.64 (dd, *J* = 13.6, 2.0 Hz, 1H), 2.58–2.27 (m, 5H), 1.92 (s, 3H), 0.97–0.92 (m, 15H). ^{13}C NMR (75 MHz, $CDCl_3$) δ: 171.8, 163.1, 143.5, 128.1, 127.8, 125.3, 88.4, 62.1, 56.3, 50.4, 48.1, 34.7, 32.9, 26.9, 16.0, 12.4. IR (thin film, cm^{-1}): 2966, 1640, 1600, 1492, 1450, 1261. HRMS (ESI): calcd for $C_{22}H_{37}O_2N_2^+$ 361.2850, found 361.2848.

10f: colorless oil, 40.3 mg, 65% yield. ^{1}H NMR (300 MHz, $CDCl_3$) δ: 9.69 (d, *J* = 10.5 Hz, 1H), 5.90–5.78 (m, 1H), 4.96–4.87 (m, 2H), 3.63 (s, 3H), 3.20 (td, *J* = 10.4, 2.1 Hz, 1H), 3.04–2.96 (m, 2H), 2.62 (dt, *J* = 13.8, 2.9 Hz, 1H), 2.55–2.26 (m, 5H), 1.94 (s, 3H), 0.98–0.90 (m, 15H). ^{13}C NMR (75 MHz, $CDCl_3$) δ: 171.4, 162.6, 139.1, 112.7, 87.2, 62.0, 56.2, 50.4, 48.1, 34.8, 31.4, 26.9, 15.6, 12.4. IR (thin film, cm^{-1}): 2968, 1640, 1601, 1452, 1265. HRMS (ESI): calcd for $C_{18}H_{35}O_2N_2^+$ 311.2693, found 311.2692.

10g: colorless oil, 50.5 mg, 78% yield. ^{1}H NMR (300 MHz, $CDCl_3$) δ: 9.20 (d, *J* = 10.6 Hz, 1H), 4.10 (q, *J* = 7.1 Hz, 2H), 3.23–3.11 (m, 1H), 2.65–2.34 (m, 6H), 2.31–2.11 (m, 4H), 1.67–1.46 (m, 4H), 1.25 (t, *J* = 7.1 Hz, 3H), 0.98–0.89 (m, 15H). ^{13}C NMR (75 MHz, $CDCl_3$) δ: 171.1, 161.1, 87.7, 60.3, 58.5, 56.5, 48.2, 34.8, 27.1, 26.9, 24.2, 23.2, 22.7, 14.9, 12.5. IR (thin film, cm^{-1}): 2966, 1643, 1600, 1455, 1235. HRMS (ESI): calcd for $C_{19}H_{37}O_2N_2^+$ 325.2850, found 325.2848.

10h: colorless oil, 11.9 mg, 20% yield. ^{1}H NMR (300 MHz, $CDCl_3$) δ: 9.50 (d, *J* = 10.2 Hz, 1H), 3.64 (s, 3H), 3.19–3.07 (m, 1H), 2.62 (dd, *J* = 13.7, 2.2 Hz, 1H), 2.58–2.18 (m, 7H), 1.79 (s, 3H), 1.10 (t, *J* = 7.7 Hz, 3H), 0.92 (dd, *J* = 12.7, 5.6 Hz, 15H). ^{13}C NMR (75 MHz, $CDCl_3$) δ: 171.9, 166.7, 83.7, 62.0, 56.8, 50.3, 48.2, 34.7, 27.0, 21.9, 12.2, 12.2, 12.0. IR (thin film, cm^{-1}): 2968, 1640, 1601, 1441, 1620. HRMS (ESI): calcd for $C_{17}H_{35}O_2N_2^+$ 299.2693, found 299.2690.

Control Reactions of Enamine 10a or 10a–TfOH with 5a. To a solution of enamine **10a** (0.30 mmol) in dried CH_2Cl_2 (10 mL) was added TfOH (0.30 mmol, 1.0 equiv) dropwise with vigorous stirring. After being stirred for 10 min, the solvent was removed under reduced pressure to give **10a**–TfOH as a white solid. To **10a** (0.10 mmol) or **10a**–TfOH (0.10 mmol), *m*-nitrobenzoic acid (1.0 equiv or none), and MeCN (0.2 mL) in a standard glass vial with stir bar was added **5a** (0.10 mmol) in one portion. The reaction was stirred at room temperature. After 60 h, the mixture was directly loaded onto a silica gel column and eluted with ethyl acetate/petroether (1:10) to give the target products.

Control Reactions of Enamine 10a or 10a–TfOH with 2a. To **10a** (0.10 mmol) or **10a**–TfOH (0.10 mmol), *m*-nitrobenzoic acid (1.0 equiv or none), and CH_2Cl_2 (0.2 mL) in a standard glass vial with stir bar was added **2a** (0.10 mmol) in one portion. The reaction was stirred at room temperature. After 30 h, the mixture was directly loaded onto silica gel column and eluted with ethyl acetate/petroether (1:3) to give the target products.

dx.doi.org/10.1021/jo502152w | J. Org. Chem. 2014, 79, 11517–11526

■ ASSOCIATED CONTENT

Supporting Information

CIF file of compound **9**, NMR spectra, and HPLC traces for the products. This material is available free of charge via the Internet at http://pubs.acs.org.

■ AUTHOR INFORMATION

Corresponding Author

*E-mail: luosz@iccas.ac.cn.

Notes

The authors declare no competing financial interest.

■ ACKNOWLEDGMENTS

We thank the Natural Science Foundation of China (21390400, 21025208 and 21202171) and the National Basic Research Program of China (2011CB808600) for financial support. S. L. is supported by the National Program of Top-notch Young Professionals and the CAS Youth Innovation Promotion Association.

■ REFERENCES

(1) For recent reviews, see: (a) Mukherjee, S.; Yang, J. W.; Hoffmann, S.; List, B. *Chem. Rev.* **2007**, *107*, 5471. (b) Melchiorre, P.; Marigo, M.; Carlone, A.; Bartoli, G. *Angew. Chem., Int. Ed.* **2008**, *47*, 6138. (c) Bertelsen, S.; Jørgensen, K. A. *Chem. Soc. Rev.* **2009**, *38*, 2178. (d) Jensen, K. L.; Dickmeiss, G.; Jiang, H.; Albrecht, Ł.; Jørgensen, K. A. *Acc. Chem. Res.* **2012**, *45*, 248.

(2) (a) Xu, C.; Zhang, L.; Luo, S. *Angew. Chem., Int. Ed.* **2014**, *53*, 4149. (b) Zhang, L.; Xu, C.; Mi, X.; Luo, S. *Chem.—Asian J.* **2014**, DOI: 10.1002/asia.201402720. (c) Zhu, Y.; Zhang, L.; Luo, S. *J. Am. Chem. Soc.* **2014**, *136*, 14642.

(3) For recent examples, see: (a) Christoffers, J.; Mann, A. *Chem.—Eur. J.* **2001**, *7*, 1014. (b) Kreidler, B.; Baro, A.; Frey, W.; Christoffers, J. *Chem.—Eur. J.* **2005**, *11*, 2660. (c) Drège, E.; Guillaume, A.; Boukhedimi, N.; Marrot, J.; Troufflard, C.; Tran Huu-Dau, M.-E.; Joseph, D.; Delarue-Cochin, S. *J. Org. Chem.* **2010**, *75*, 7596. (d) Fujimoto, T.; Endo, K.; Tsuji, H.; Nakamura, M.; Nakamura, E. *J. Am. Chem. Soc.* **2008**, *130*, 4492.

(4) Wagner, J.; Lerner, R. A.; Barbas, C. F., III. *Science* **1995**, *270*, 1797.

(5) For reviews on primary amine catalysis, see: (a) Melchiorre, P. *Angew. Chem., Int. Ed.* **2012**, *51*, 9748. (b) Jiang, L.; Chen, Y.-C. *Catal. Sci. Technol.* **2011**, *1*, 354. (c) Xu, L.-W.; Luo, J.; Lu, Y. *Chem. Commun.* **2009**, 1807. (d) Chen, Y.-C. *Synlett* **2008**, 1919. (e) Bartoli, G.; Melchiorre, P. *Synlett* **2008**, 1759.

(6) For recent examples, see: (a) Luo, S.; Xu, H.; Li, J.; Zhang, L.; Cheng, J.-P. *J. Am. Chem. Soc.* **2007**, *129*, 3074. (b) Luo, S.; Xu, H.; Chen, L.; Cheng, J.-P. *Org. Lett.* **2008**, *10*, 1775. (c) Luo, S.; Xu, H.; Zhang, L.; Li, J.; Cheng, J.-P. *Org. Lett.* **2008**, *10*, 653. (d) Luo, S.; Qiao, Y.; Zhang, L.; Li, J.; Li, X.; Cheng, J.-P. *J. Org. Chem.* **2009**, *74*, 9521. (e) Luo, S.; Zhou, P.; Li, J.; Cheng, J.-P. *Chem.—Eur. J.* **2010**, *16*, 4457. For an account, see: (f) Zhang, L.; Luo, S. *Synlett* **2012**, *23*, 1575.

(7) (a) Juhl, K.; Jørgensen, K. A. *J. Am. Chem. Soc.* **2002**, *124*, 2420. (b) Marigo, M.; Juhl, K.; Jørgensen, K. A. *Angew. Chem., Int. Ed.* **2003**, *42*, 1367. (c) Ma, S.; Jiao, N.; Zheng, Z.; Ma, Z.; Lu, Z.; Ye, L.; Deng, Y.; Chen, G. *Org. Lett.* **2004**, *6*, 2193. (d) Bernardi, L.; Zhuang, W.; Jørgensen, K. A. *J. Am. Chem. Soc.* **2005**, *127*, 5772. (e) Foltz, C.; Stecker, B.; Marconi, G.; Bellemin-Laponnaz, S.; Wadepohl, H.; Gade, L. H. *Chem. Commun.* **2005**, 5115. (f) Kim, S. M.; Kim, H. R.; Kim, D. Y. *Org. Lett.* **2005**, *7*, 2309. (g) Kang, Y. K.; Kim, D. Y. *Tetrahedron Lett.* **2006**, *47*, 4565. (h) Huber, D. P.; Stanek, K.; Togni, A. *Tetrahedron: Asymmetry* **2006**, *17*, 658. (i) Comelles, J.; Pericas, À.; Moreno-Mañas, M.; Vallribera, A.; Drudis-Solé, G.; Lledos, A.; Parella, T.; Roglans, A.; García-Grands, S.; Roces-Fernández, L. *J. Org. Chem.* **2007**, *72*, 2077. (j) Mashiko, T.; Hara, K.; Tanaka, D.; Fujiwara, Y.; Kumagai, N.; Shibasaki, M. *J. Am. Chem. Soc.* **2007**, *129*, 11342. (k) Mashiko, T.; Kumagai, N.; Shibasaki, M. *Org. Lett.* **2008**, *10*, 2725. (l) Hasegawa, Y.; Watanabe, M.; Gridnev, I. D.; Ikariya, T. *J. Am. Chem. Soc.* **2008**, *130*, 2158. (m) Gaab, M.; Bellemin-Laponnaz, S.; Gade, L. H. *Chem.—Eur. J.* **2009**, *15*, 5450. (n) Pericas, À.; Shafir, A.; Vallribera, A. *Org. Lett.* **2013**, *15*, 1448.

(8) (a) Saaby, S.; Bella, M.; Jørgensen, K. A. *J. Am. Chem. Soc.* **2004**, *126*, 8120. (b) Pihko, P. M.; Pohjakallio, A. *Synlett* **2004**, 2115. (c) Liu, X.; Li, H.; Deng, L. *Org. Lett.* **2005**, *7*, 167. (d) Terada, M.; Nakano, M.; Ube, H. *J. Am. Chem. Soc.* **2006**, *128*, 16044. (e) Xu, X.; Yabuta, T.; Yuan, P.; Takemoto, Y. *Synlett* **2006**, 137. (f) Jung, S. H.; Kim, D. Y. *Tetrahedron Lett.* **2008**, *49*, 5527. (g) Konishi, H.; Lam, T. Y.; Malerich, J. P.; Rawal, V. H. *Org. Lett.* **2010**, *12*, 2028. (h) Inokuma, T.; Furukawa, M.; Uno, T.; Suzuki, Y.; Yoshida, K.; Yano, Y.; Matsuzaki, K.; Takemoto, Y. *Chem.—Eur. J.* **2011**, *17*, 10470. (i) Zhang, Z.-H.; Dong, X.-Q.; Tao, H.-Y.; Wang, C.-J. *ARKIVOC* **2011**, 137.

(9) (a) He, R.; Wang, X.; Hashimoto, T.; Maruoka, K. *Angew. Chem., Int. Ed.* **2008**, *47*, 9466. (b) Lan, Q.; Wang, X.; He, R.; Maruoka, K. *Tetrahedron Lett.* **2009**, *50*, 3280.

(10) Liu, X.; Sun, B.; Deng, L. *Synlett* **2009**, 1685.

(11) (a) Xu, C.; Zhang, L.; Zhou, P.; Luo, S.; Cheng, J.-P. *Synthesis* **2013**, *45*, 1939. (b) Zhou, P.; Zhang, L.; Luo, S.; Cheng, J.-P. *J. Org. Chem.* **2012**, *77*, 2526.

(12) There is only one organocatalystic example with α-unsubstituted β-ketoesters: Halland, N.; Abured, P. S.; Jørgensen, K. A. *Angew. Chem., Int. Ed.* **2004**, *43*, 1272.

(13) For base-catalyzed Robinson annulation, see: Kubo, H.; Kozawa, I.; Takao, K.-i. *Tetrahedron Lett.* **2008**, *49*, 1203.

(14) For selected examples of Lewis acid catalyzed Michael reaction, see: (a) Sasai, H.; Arai, T.; Satow, Y.; Houk, K. N.; Shibasaki, M. *J. Am. Chem. Soc.* **1995**, *117*, 6194. (b) Sasai, H.; Shibasaki, M. *Tetrahedron Lett.* **1996**, *37*, 5561. (c) Hamashima, Y.; Hotta, D.; Sodeoka, M. *J. Am. Chem. Soc.* **2002**, *124*, 11240. (d) Hamashima, Y.; Takano, H.; Hotta, D.; Sodeoka, M. *Org. Lett.* **2003**, *5*, 3225. (e) Nour, M.; Tan, K.; Jankowski, R.; Cavé, C. *Tetrahedron: Asymmetry* **2001**, *12*, 765.

(15) Frisch, M. J. et al. *Gaussian 09, Revision A. 01*; Gaussian, Inc., Wallingford, CT, 2009.

(16) (a) Zhao, Y.; Truhlar, D. G. *Acc. Chem. Res.* **2008**, *41*, 157. (b) Zhao, Y.; Truhlar, D. G. *Theor. Chem. Acc.* **2008**, *120*, 215.

(17) (a) Marenich, A. V.; Cramer, C. J.; Truhlar, D. G. *J. Phys. Chem. B* **2009**, *113*, 6378. (b) Ribeiro, R. F.; Marenich, A. V.; Cramer, C. J.; Truhlar, D. G. *J. Phys. Chem. B* **2011**, *115*, 14556.

(18) (a) Pierce, M. D.; Johnston, R. C.; Mahapatra, S.; Yang, H.; Carter, R. G.; Cheong, P. H.-Y. *J. Am. Chem. Soc.* **2012**, *134*, 13624. (b) Yang, H.; Carter, R. G. *Org. Lett.* **2010**, *12*, 3108.

(19) Kalaitzakis, D.; Kambourakis, S.; Rozzell, J. D.; Smonou, I. *Tetrahedron: Asymmetry* **2007**, *18*, 2418.

(20) Gao, L.; Kang, B. C.; Hwang, G.-S.; Ryu, D. H. *Angew. Chem., Int. Ed.* **2012**, *51*, 8322.

(21) Toda, F.; Suzuki, T.; Higa, S. *J. Chem. Soc., Perkin Trans. 1* **1998**, 3521.